

Supplementary Information

Fabrication of silicon nanowire arrays by near-field laser ablation and metal-assisted chemical etching

D Brodoceanu¹, H Z Alhmoud², R Elnathan², B Delalat², N H Voelcker² and T Kraus¹

¹ INM-Leibniz Institute for New Materials, Saarbruecken 66123, Campus D2 2, Germany,

² ARC Centre of Excellence in Convergent Bio-Nano Science and Technology, Mawson Institute, University of South Australia, Adelaide, SA 5001, Australia

E-mails: daniel.brodoceanu@leibniz-inm.de, tobias.kraus@leibniz-inm.de

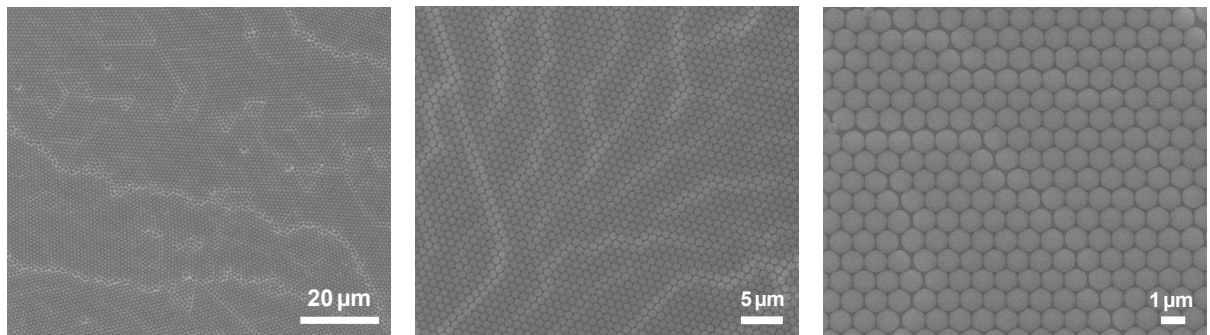


Figure S1. Typical Scanning Electron Microscopy (SEM) of monolayers of PS microspheres assembled on gold-coated silicon surface.

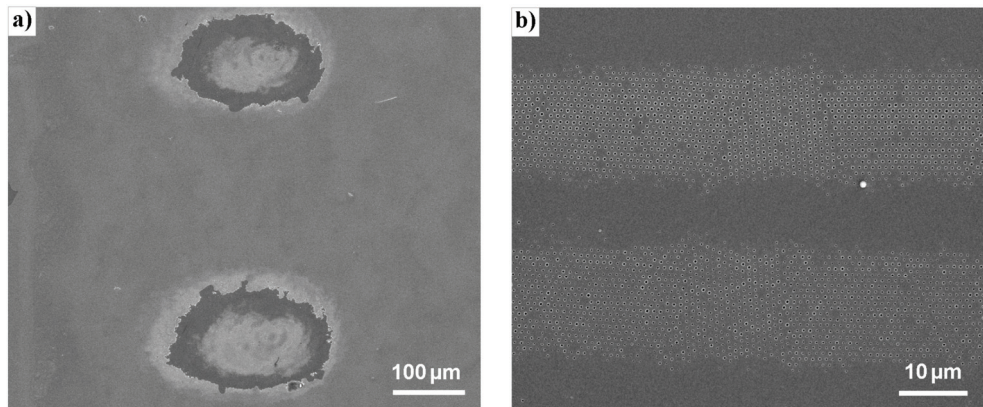


Figure S2. Laser spots produced by irradiation of the microsphere monolayer self-assembled on the gold-coated silicon. (a) Tilted SEM micropgraph showing round spots produced using a spherical lens with focal distance of 5 cm. Hole arrays formed on gold layer at the periphery of the spots, due to Gaussian profile of the laser beam (b) Linear spots produced with a cylindrical lens with focal distance of 5 cm.

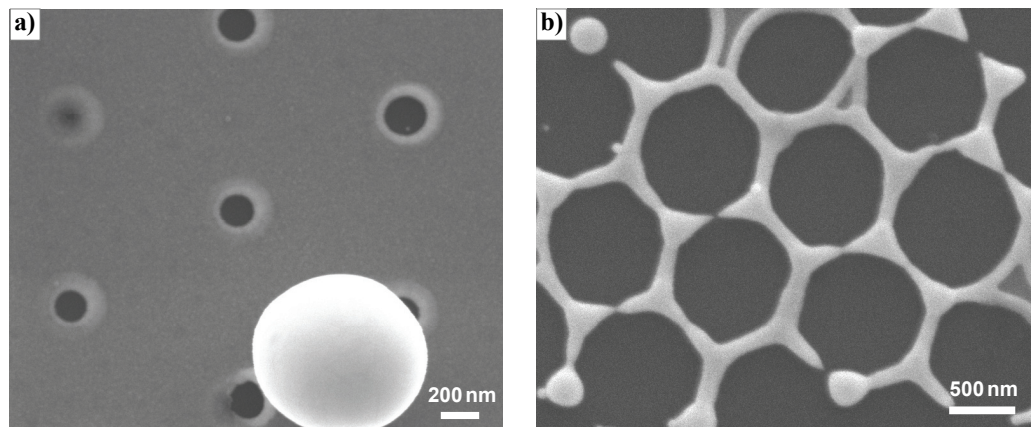


Figure S3. Hexagonal pattern of holes achieved in 30 nm gold layer using PS microspheres with diameter of 1 μm laser irradiated under extreme fluence conditions. (a) Smallest holes (~ 160 nm) observed at a fluence of $\phi \approx 11$ mJ/cm². (b) Maximum fluence ($\phi \approx 55$ mJ/cm²) at which the resulting metal structure still retains the hexagonal pattern of the original monolayer.

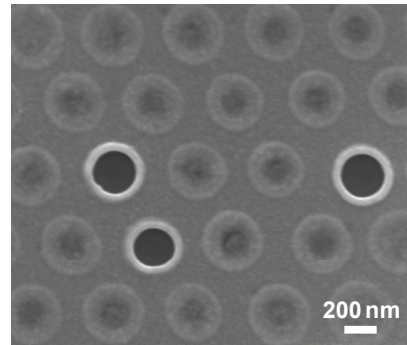


Figure S4. Patterning of 30 nm gold layer by single-pulse laser irradiation of self-assembled PS microspheres with diameter of 500 nm.

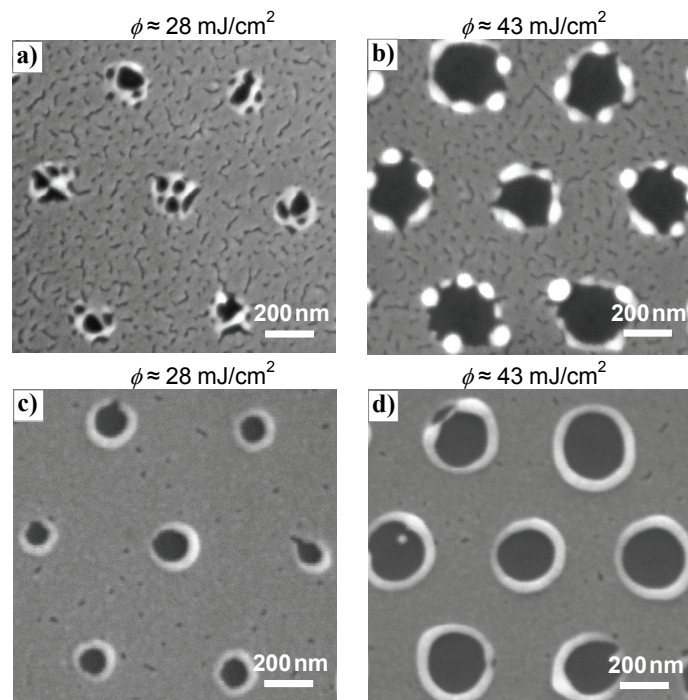


Figure S5. The influence of metal surface morphology on the hole formation. (a-b) SEM micrographs of the holes generated at two different laser fluences in 20 nm thick gold layer with preexisting cracks on its surface. The cracks disrupted the flow of the laser-induced heat at the near-field spot. (c-d) Holes generated in an almost crack-free gold layer.

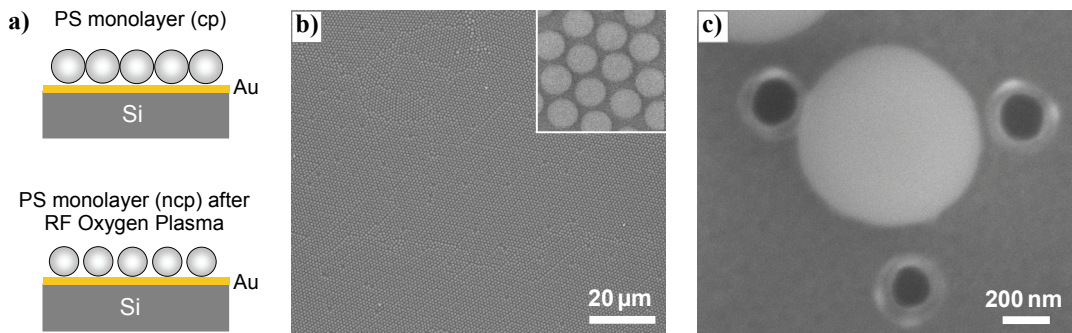


Figure S6. Tuning the PS microsphere diameter using an RF oxygen plasma. (a) Schematic illustration of a close-packed (cp) monolayer of PS microspheres treated with RF oxygen plasma. (b) SEM image of a hexagonal non-close packed (ncp) array of microspheres with diameter of $750 \text{ nm} \pm 15 \text{ nm}$ obtained after 12 min etching a cp monolayer of $1 \mu\text{m}$ PS microspheres in oxygen plasma ($P = 50\text{W}$). The inset shows a close-up view of the ncp array. (c) Hole array in gold layer after single-pulse laser irradiation ($\lambda = 355 \text{ nm}$, $\tau = 10 \text{ ns}$, $\phi \approx 18 \text{ mJ/cm}^2$) using the etched PS microspheres as microlenses.

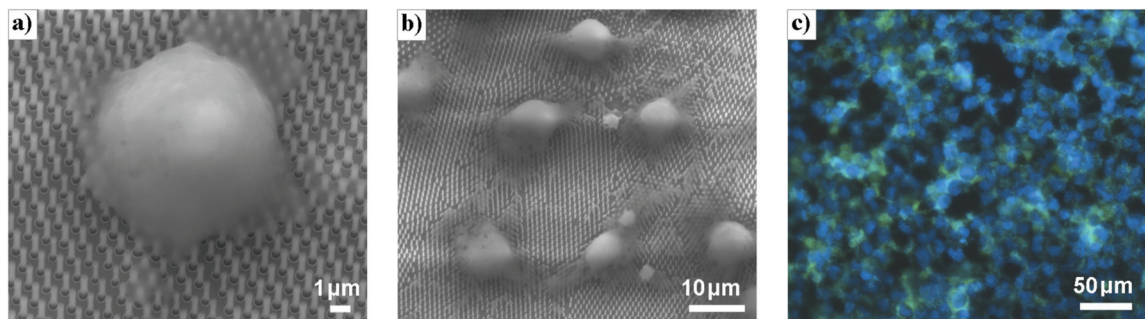


Figure S7. Cell transfection of HEK 293 cells using VA-SiNW. (a-b) Scanning electron micrographs of the interaction between HEK 293 cells and laser fabricated VA-SiNW arrays. (c) Fluorescence image of transfected HEK293. The nanowires were $280 \text{ nm} \pm 25 \text{ nm}$ in diameter, $1.55 \mu\text{m}$ in length, with an array density of $1 \text{ NW}/\mu\text{m}^2$.